

# Kinetics of Volume Phase Transition in Nematic Gels Coupled with Nematic–Isotropic Phase Transition

Kenji Urayama,\* Yuko O. Arai, and Toshikazu Takigawa

Department of Material Chemistry, Kyoto University, Nishikyo-ku, Kyoto 615-8510, Japan

Received April 28, 2004

**ABSTRACT:** We have investigated the dynamics of the phase transition between swollen isotropic and shrunken nematic states for a nematic network swollen in nematic solvent. The kinetics of swelling and shrinking driven by temperature ( $T$ )-jumps across the nematic–isotropic ( $N$ – $I$ ) transition temperature ( $T_{NI}^G$ ) strongly depends on the distance of destination temperature ( $T_d$ ) from  $T_{NI}^G$  ( $\Delta T$ ). When  $T_d$  is far above  $T_{NI}^G$ , the  $N \rightarrow I$  transition completes fast within the  $T$ -jump, which yields the swelling process of totally isotropic gel without coupling of  $N \rightarrow I$  transition. If  $T_d$  is moderately above  $T_{NI}^G$ , the  $N \rightarrow I$  transition slowly proceeds from surface toward center of gel with accompanying swelling. In this case, the total swelling process is composed of two different stages, i.e., during  $N \rightarrow I$  transition and after  $N \rightarrow I$  transition: The former is a thermally activated process strongly coupled with  $N \rightarrow I$  transition; the latter is the  $T$ -independent swelling process of totally isotropic gel. When the  $T$ -quench from isotropic phase to nematic phase is sufficiently deep, the  $I \rightarrow N$  transition and shrinking proceed uniformly whereas the process is decelerated with increasing the degree of total volume change. In the case of  $T_d$  slightly above (or below)  $T_{NI}^G$ , the onset of the  $N \rightarrow I$  (or  $I \rightarrow N$  transition) is governed by heterogeneous nucleation, and the following growth of the nuclei yields considerably nonuniform swelling (or shrinking). The resulting dynamics becomes markedly slower than that observed after the  $T$ -jumps with sufficiently large  $\Delta T$ .

## Introduction

Polymer networks with nematicity (nematic networks) have attracted much attention because of their hybrid characters possessing the properties of polymer network and nematic liquid crystal (LC).<sup>1,2</sup> Recently, we experimentally found that nematic networks swollen in low molecular mass LCs or isotropic (nonmesomorphic) solvents undergo a discontinuous volume transition induced by the nematic–isotropic ( $N$ – $I$ ) phase transition.<sup>3,4</sup> The swollen isotropic network is discontinuously and thermoreversibly changed into the shrunken nematic network at a characteristic temperature ( $T_{NI}^G$ ). The volume transition of nematic gels is triggered by the  $N$ – $I$  transition and thus substantially different from that of isotropic gels caused by the balance between attractive and repulsive molecular forces acting on networks. We elucidated equilibrium properties of the volume transition phenomena of nematic gels<sup>3–6</sup> and also demonstrated that the results were successfully described by a mean-field theory.<sup>7,8</sup> However, the dynamics of volume phase transition of nematic gels has not yet been investigated.

So far, the effect of nematic ordering on phase separation dynamics in LC polymer/solvent systems or LC polymer blends has been studied by many researchers.<sup>9–14</sup> In these systems or usual bulk LCs, the total compositions are fixed throughout the  $N$ – $I$  transition process. Of importance is that, unlike these systems, a nematic gel with surrounding solvent is a thermodynamically semiopen system which allows the change in solvent (or network) content inside the gel during the  $N$ – $I$  transition. This process is driven by swelling or shrinking of network, i.e., collective diffusion of network. Such coupling of the  $N$ – $I$  transition and collective diffusion of the network is expected to yield a

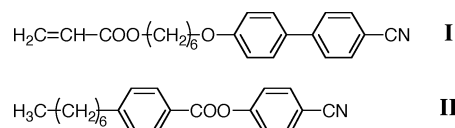


**Figure 1.** Molecular structures of the employed liquid crystalline monomer and solvent.

new interesting phenomenon absent in dynamics of familiar volume transitions of nonmesomorphic gels<sup>15–20</sup> as well as  $N$ – $I$  transitions of LC systems with fixed compositions.<sup>9–14</sup> In addition, to understand swelling and shrinking kinetics of nematic gels is important for application to industrial devices such as actuators. Yurif et al.<sup>21</sup> reported the swelling kinetics of nematic networks in nematic solvents, but they focused only on the swelling process from the dry nematic state to the swollen nematic state without  $N$ – $I$  transition. In the present study, we have investigated dynamics of swelling and shrinking of nematic gels respectively induced by  $N \rightarrow I$  and  $I \rightarrow N$  transitions after  $T$ -jumps across  $T_{NI}^G$ . The swelling and shrinking kinetics of a nematic gel within isotropic phase or nematic phase without  $N$ – $I$  transition has also been studied as a basis to discuss the kinetics of volume transition accompanying  $N$ – $I$  transition.

## Experimental Section

A side-chain LC network (LCN-A or LCN-B) was prepared by radical polymerization of the mesogenic acrylate monomer **I** (Figure 1) with 1,6-hexanediol diacrylate (cross-linker). 2,2'-Azobis(isobutyronitrile) was employed as an initiator. The molar fractions of **I**, cross-linker, and initiator were 98, 1, and 1 mol %, respectively. The cross-linking reaction was carried out in a capillary with diameter of several hundred microns at 80 °C where the monomer **I** was in the isotropic phase. The details of the sample preparation were described elsewhere.<sup>5</sup> After a washing procedure, the dried cylindrical gel was immersed in the low molecular mass liquid crystal **II** (Figure 1) with  $N$ – $I$  transition temperature of 54.2 °C. The  $N$ – $I$

\* To whom correspondence should be addressed. E-mail: urayama@rheogate.polym.kyoto-u.ac.jp.

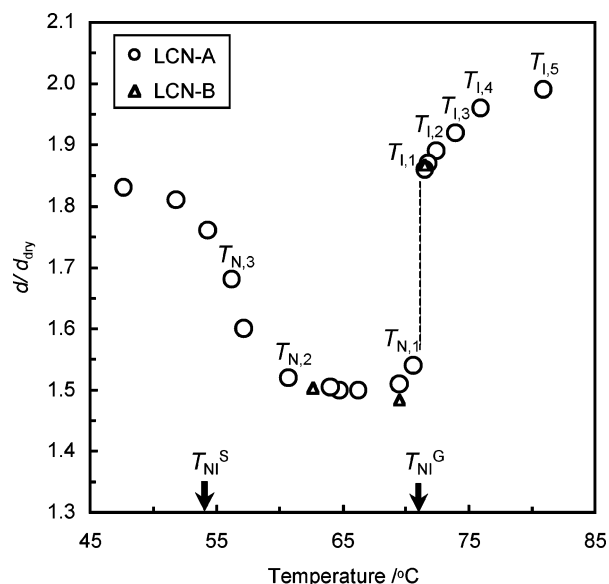


**Figure 2.** Temperature dependence of the diameter ratio  $d/d_{\text{dry}}$  of the cylindrical nematic network LCN-A swollen in the nematic solvent.  $d$  and  $d_{\text{dry}}$  denote the gel diameters in equilibrium swollen and dry states, respectively.  $T_{\text{NI}}^{\text{G}}$  and  $T_{\text{NI}}^{\text{S}}$  indicate the nematic–isotropic transition temperature inside gel and that for the pure solvent outside gel, respectively. There exists no appreciable difference in  $d$  between heating and cooling processes.  $T_{i,1}$  ( $i = 1-5$ ) and  $T_{N,1}$  ( $i = 1-3$ ) correspond to the destination temperatures employed in  $T$ -jump experiments. The triangular symbols represent the data of the sample LCN-B (separately prepared but with the same condition as LCN-A) used for the additional experiment.

transition temperature of the dry LC network measured on cooling was 131 °C.

The processes of swelling and shrinking of the gel after  $T$ -jumps varying in initial and destination temperatures (designated as  $T_i$  and  $T_d$ , respectively) were observed by a polarizing optical microscope (Nikon E600 POL) equipped with a temperature-controllable sample stage (Mettler FP-82) under a nitrogen atmosphere. The surface level of the solvent in an optical cell was low enough so that the phase of the gel and the boundary of the gel surface were clearly visible when viewed through the microscope (but high enough to immerse the gel completely). The equilibrium swollen gel at  $T_i$  was heated or cooled to  $T_d$  with the rate 1.0 °C/min, which was enough slow to avoid appreciable overshoot or undershoot in temperature around  $T_d$ . The heating and cooling from  $T_i$  toward  $T_d$  required a finite time, but it was negligibly short compared with the time scale of the whole course concerned here. Both swelling and shrinking proceeded isotropically even in the nematic phase due to a polydomain nematic structure without global orientation of director. Accordingly, gel volume in the swelling or shrinking process was assumed to be proportional to the cube of gel diameter.

Almost all experiments were carried out using the network sample LCN-A. For only two runs in an additional experiment, we used the network sample LCN-B which was prepared separately but with the same conditions as LCN-A. Hereafter the description is for the data obtained for LCN-A unless specified otherwise.

## Results and Discussion

**Equilibrium Swelling-Temperature Phase Diagram.** The temperature ( $T$ ) dependence of the gel diameter in equilibrium swollen state ( $d$ ) is depicted in Figure 2, where  $d$  is reduced by the gel diameter in dry state ( $d_{\text{dry}} = 216 \mu\text{m}$ ).<sup>22</sup> The results were essentially the same as reported in our previous paper.<sup>3</sup> The temperatures  $T_{\text{NI}}^{\text{G}}$  and  $T_{\text{NI}}^{\text{S}}$  denote the N–I transition temperature inside the gel (i.e., for the swollen gel) and that

for the surrounding pure solvent, respectively. There exist three characteristic temperature regions depending on the phase of each LC: totally isotropic phase ( $T > T_{\text{NI}}^{\text{G}}$ ); nematic phase inside the gel and isotropic phase outside the gel ( $T_{\text{NI}}^{\text{G}} > T > T_{\text{NI}}^{\text{S}}$ ); totally nematic phase ( $T < T_{\text{NI}}^{\text{S}}$ ). As seen in the figure, upon cooling to  $T_{\text{NI}}^{\text{G}}$ , the swollen isotropic gel is discontinuously transformed into the shrunken nematic gel. At temperatures below  $T_{\text{NI}}^{\text{G}}$ , the nematic network and the nematic solvent inside the gel form a single nematic phase. In the region  $T_{\text{NI}}^{\text{G}} > T > 60$  °C, the swelling degree of the shrunken nematic gel is almost constant, and it increases again with descending  $T$  in the region  $60$  °C  $> T > T_{\text{NI}}^{\text{S}}$ . The nematic ordering of the solvent outside the gel at  $T_{\text{NI}}^{\text{S}}$  yields an inflection on the swelling curve without discontinuity. There was no appreciable difference in  $d$  between heating and cooling processes as reported before.<sup>3</sup> A slight thermal hysteresis effect on  $T_{\text{NI}}^{\text{G}}$  was observed: Each of  $T_{\text{NI}}^{\text{G}}$  in heating and cooling processes is 71.2 and 70.9 °C, respectively. Hereafter we use  $T_{\text{NI}}^{\text{G}}$  according to the temperature variation concerned without notification. In the figure,  $T_{\text{NI}}^{\text{G}}$  in cooling process is indicated. The data for LCN-B used in the additional experiment are also shown in the figure, and  $T_{\text{NI}}^{\text{G}}$  for LCN-B upon cooling is 70.4 °C.

We have investigated the dynamics of the phase transition between the swollen isotropic and shrunken nematic states driven by the  $T$ -jumps across  $T_{\text{NI}}^{\text{G}}$  on heating or cooling. The swelling and shrinking kinetics within isotropic phase ( $T > T_{\text{NI}}^{\text{G}}$ ) or nematic phase ( $T_{\text{NI}}^{\text{S}} < T < T_{\text{NI}}^{\text{G}}$ ) of gel without the N–I transition has also been examined. It should be noticed that the phase of the surrounding solvent outside the gel is isotropic throughout all measurements because the temperature range concerned here is above  $T_{\text{NI}}^{\text{S}}$ .

**Swelling and Shrinking Kinetics within Isotropic Phase or Nematic Phase.** In this section, we describe the swelling and shrinking kinetics within isotropic phase or nematic phase without the N–I transition. Figure 3a illustrates the time ( $t$ ) dependence of gel diameter in swelling or shrinking process within nematic phase after the  $T$ -jump of  $66.2 \rightarrow 57.2$  °C or  $57.2 \rightarrow 66.2$  °C, respectively. The swelling or shrinking equilibrium is achieved at  $t \approx 9 \times 10^3$  s or  $t \approx 2 \times 10^4$  s, respectively. In Figure 3b, the ratio  $\Delta d(t)/\Delta d$  for the data in Figure 3a is plotted as a function of  $t$  in a semilog scale. The quantities  $\Delta d(t)$  and  $\Delta d$  are defined as

$$\Delta d(t) = d_{\infty} - d(t) \quad (1)$$

$$\Delta d = d_{\infty} - d_0 \quad (2)$$

where  $d_{\infty}$  and  $d_0$  denote the equilibrium diameters before and after  $T$ -jump, in other words, the  $d$  values at  $T_d$  and  $T_i$ , respectively. The data for each process fall on a straight line passing near the origin, indicating that the diameter (or volume) change is approximated by a single-exponential relaxation process. The characteristic time  $\tau$  for the swelling or shrinking process is evaluated from the inverse of each slope as  $\tau = 2.99 \times 10^3$  s or  $\tau = 6.57 \times 10^3$  s, respectively. From the values of  $\tau$  and  $d_{\infty}$ , the collective diffusion constant  $D$  is evaluated using the following relation for cylindrical gels:<sup>23</sup>

$$D = \frac{d_{\infty}^2}{24\tau} \quad (3)$$

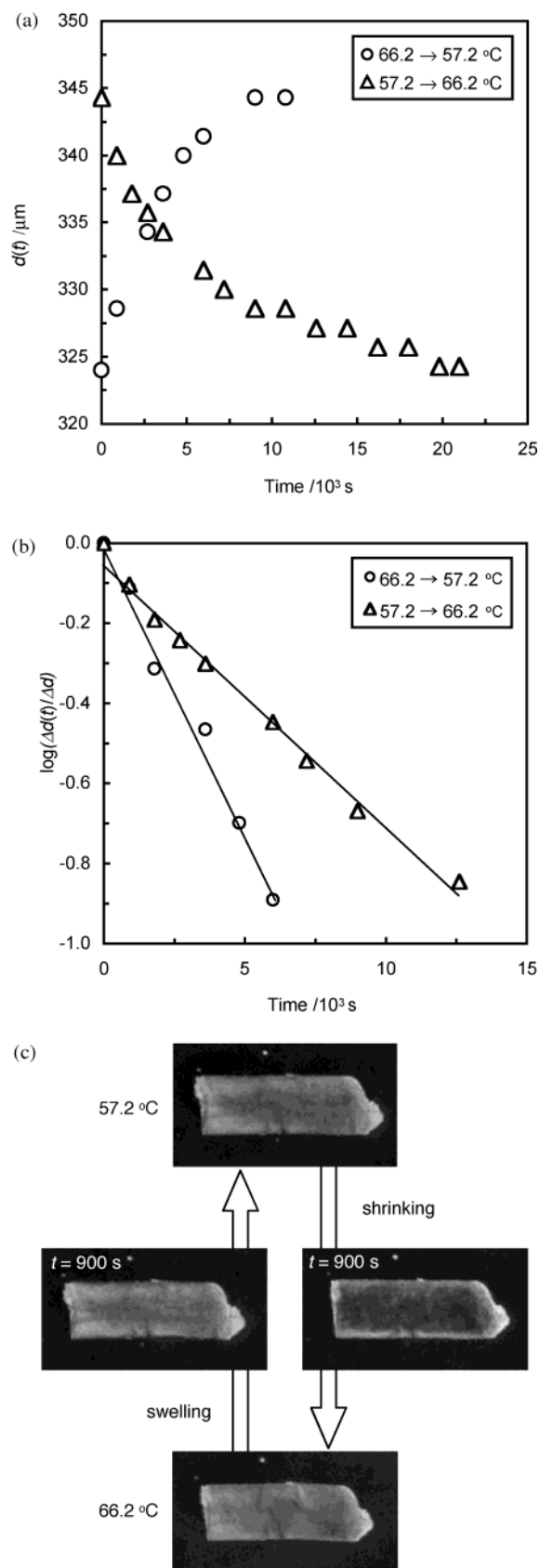


**Figure 3.** Swelling and shrinking processes within nematic phase after  $T$ -jumps of  $66.2 \rightarrow 57.2$  °C and  $57.2 \rightarrow 66.2$  °C, respectively: (a) time dependence of gel diameter; (b) semilog plot of the ratio  $\Delta d(t)/\Delta d$  vs time; (c) optical micrographs of the cylindrical gel under the cross-polarized condition.

As a measure of volume change upon swelling or shrinking, a volume strain  $\gamma_V$  is defined by

$$\gamma_V = \frac{V_0 - V_\infty}{V_\infty} \quad (4)$$

where  $V_0$  and  $V_\infty$  are the equilibrium volumes of gel at  $T_i$  and  $T_d$  (i.e., before and after  $T$ -jump), respectively. As is evident from the definition,  $\gamma_V$  becomes positive (negative) in shrinking (swelling). The swelling and shrinking processes within isotropic phase after the  $T$ -jumps of  $71.5 \rightarrow 80.9$  °C and  $80.9 \rightarrow 71.5$  °C, respectively, were analyzed in the same manner, although the data are not shown here. The evaluated values of  $\tau$ ,  $D$ , and  $\gamma_V$  for each process are listed in Table 1.

Of interest is that in nematic phase,  $D$  ( $= 6.66 \times 10^{-9}$  cm<sup>2</sup>/s), for shrinking is significantly smaller than  $D$  ( $= 1.64 \times 10^{-8}$  cm<sup>2</sup>/s) for swelling. The similar trend is also observed for the results in isotropic phase, but the difference in  $D$  between shrinking and swelling is much smaller than that in nematic phase. Figure 3c displays the optical micrographs under the cross-polarized condition for the cylindrical gel in the corresponding swelling and shrinking processes within nematic phase. Volume change of nematic gel causes a change in solvent content inside gel, which can induce the re-formation of the single nematic phase composed of nematic network and nematic solvent inside gel. The cross-polarized image of the gel remains bright throughout the swelling process. Meanwhile, in the case of shrinking, it becomes fairly dark at the early stage and becomes brighter again with further shrinking; the un-crossed-polarized images (which are not shown here) remain opaque throughout the shrinking process. This indicates that a structure with less nematic order inside the gel forms at the initial stage of shrinking; thereafter, a single nematic phase with developed nematic order appears again with further shrinking. In general LC systems, a decrease (or increase) of temperature in the nematic phase yields an increase (or a decrease) in nematic order of LC molecules.<sup>24,25</sup> Importantly, no appreciable change in the cross-polarized image of the nematic gel was observed upon heating and cooling in the range from 60.7 to 69.5 °C where the swelling degree exhibits no significant change in response to temperature variation. This means that the structure with less nematic order observed in the initial shrinking process is primarily caused by a concentration change of gel but not by a temperature change. It is known for the temperature-sensitive isotropic gels undergoing a discontinuous volume transition that the concentration distribution in gel during shrinking is considerably larger than that during swelling; such large concentration distribution yields a phase separation in gel, which markedly decelerates the shrinking process.<sup>16–20</sup> The appearance of the structure with less nematic order will result from a finite concentration distribution induced by shrinking, although the corresponding volume change is small. Equilibration of shrinking of nematic gel is significantly retarded by the re-formation process of the single nematic phase with developed nematic order.

**Kinetics of Swelling Induced by N  $\rightarrow$  I Transition.** We describe here the transition dynamics from the shrunken nematic gel to the swollen isotropic gel. The initial temperature was fixed at  $T_i = T_{NI}^G - 1.7$  °C. The distance of the destination temperature ( $T_d$ ) from  $T_{NI}^G$  ( $\Delta T$ ) was varied as  $\Delta T = +0.3, +1.2, +2.7, +4.7$ , and  $+9.7$  °C, and the corresponding  $T_d$  was designated as  $T_{i,i}$  ( $i = 1-5$ ) in order of  $\Delta T$  as indicated in Figure 2.

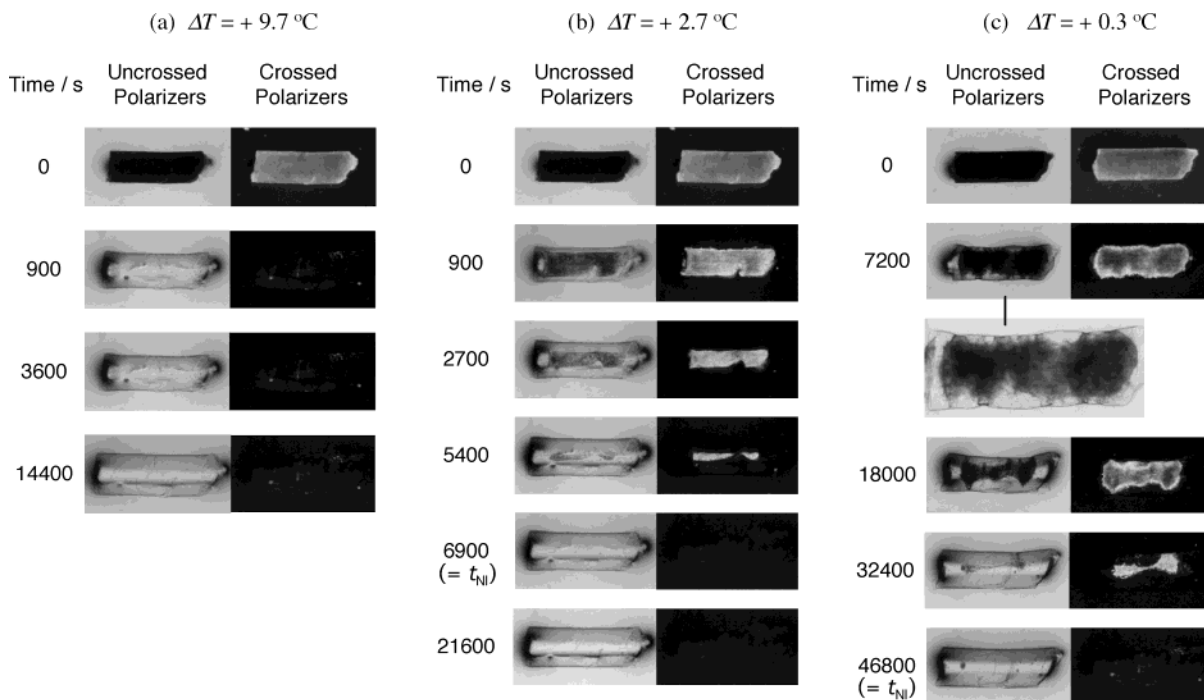


**Figure 4.** Optical micrographs of the gel in swelling processes accompanying the N  $\rightarrow$  I transition after  $T$ -jumps varying in the distance of  $T_d$  from  $T_{NI}^G$  ( $\Delta T$ ): (a)  $\Delta T = +9.7$  °C; (b)  $\Delta T = +2.7$  °C; (c)  $\Delta T = +0.3$  °C. The nematic phase completely disappears at  $t_{NI}$ . In (a), the N  $\rightarrow$  I transition completes within the  $T$ -jump. In (c), the outline of the gel as well as the boundary between nematic and isotropic domains is markedly rough particularly at the early stage, as shown in the enlarged photograph.

**Table 1. Sample Code, Initial Temperature ( $T_i$ ), Destination Temperature ( $T_d$ ), Distance of  $T_d$  from  $T_{NI}^G$  ( $\Delta T$ ), Volume Strain ( $\gamma_V$ ), Characteristic Time ( $\tau$ ), Diffusion Constant ( $D$ ), and Time at Completion of N  $\rightarrow$  I or I  $\rightarrow$  N Transition ( $t_{NI}$  or  $t_{IN}$ , Respectively) in  $T$ -Jump Experiments**

sample	phase	$T_i$ /°C	$T_d$ /°C	$\Delta T$ /°C	$\gamma_V^b$	$\tau/10^3$ s	$D/10^{-9}$ cm $^2$ s $^{-1}$	$t_{NI}$ or $t_{IN}/10^3$ s
LCN-A	I $\rightarrow$ I	80.9	71.5	0.6	0.153	3.57	18.9	
		71.5	80.9	9.7	-0.132	3.25	23.8	
	N $\rightarrow$ N	66.2	57.2	-13.7	-0.164	2.99	16.4	
		57.2	66.2	-5.0	0.197	6.57	6.66	
	N $\rightarrow$ I	69.5	71.5	0.3	-0.485	16.0	4.30	46.8
		69.5	72.4	1.2	-0.532	5.39 <sup>c</sup>	12.0 <sup>c</sup>	14.4
						3.67 <sup>d</sup>	19.0 <sup>d</sup>	
		69.5	73.9	2.7	-0.549	2.46 <sup>c</sup>	25.8 <sup>c</sup>	6.90
						3.66 <sup>d</sup>	19.8 <sup>d</sup>	
		69.5	75.9	4.7	-0.558	1.07 <sup>c</sup>	56.2 <sup>c</sup>	2.70
						3.65 <sup>d</sup>	20.7 <sup>d</sup>	
		69.5	80.9	9.7	-0.581	3.30	23.5	<sup>e</sup>
	I $\rightarrow$ N	71.5	70.6	-0.3	0.914	36.5	1.26	90.0
		71.5	64.0	-6.9	0.974	9.38	4.70	28.8
		71.5	56.2	-14.7	0.341	7.62	7.13	21.6
		71.5	69.5	-0.9	0.995	15.2	2.81	46.8
LCN-B	I $\rightarrow$ N	71.5	62.6	-7.8	0.917	16.5	2.65	57.6

<sup>a</sup>  $\Delta T = T_d - T_{NI}^G$ . <sup>b</sup> Defined by eq 4. <sup>c</sup> For the region  $t < t_{NI}$ . <sup>d</sup> For the region  $t > t_{NI}$ . <sup>e</sup> N  $\rightarrow$  I transition completes during  $T$ -jump.

The transition dynamics observed is qualitatively classified into the three types, depending on  $\Delta T$ : (i)  $T_d$  far from  $T_{NI}^G$  ( $T_{I,5}$ ); (ii)  $T_d$  moderately close to  $T_{NI}^G$  ( $T_{I,2}$ ,  $T_{I,3}$ ,  $T_{I,4}$ ); (iii)  $T_d$  slightly above  $T_{NI}^G$  ( $T_{I,1}$ ).

Parts a, b, and c in Figure 4 display the optical micrographs for the swelling processes in the cases i, ii, and iii, respectively. As shown in Figure 4a, the N  $\rightarrow$  I transition at  $T_{I,5}$  proceeds so fast that it completes within the  $T$ -jump. The phase of the gel is totally isotropic throughout the swelling process after the temperature reaches  $T_d$ . The  $t$  dependence of gel diameter and a semilog plot of  $\Delta d(t)/\Delta d$  vs  $t$  for this swelling process are illustrated in parts a and b of Figure 5, respectively. In Figure 5b, all data fall on a straight line, and the slope of the line yields  $\tau = 3.30 \times 10^3$  s. The estimated value of  $D (= 2.35 \times 10^{-8}$  cm $^2$ /s) well accords with  $D (= 2.38 \times 10^{-8}$  cm $^2$ /s) for the swelling within

isotropic phase, clearly indicating that the  $T$ -jumps to the temperatures far above  $T_{NI}^G$  (case i) yield the swelling process of isotropic gel without coupling of the N  $\rightarrow$  I transition.

When  $T_d$  is moderately close to  $T_{NI}^G$  (case ii), the swelling coupled with the N  $\rightarrow$  I transition appears as shown in Figure 4b. The progress of the N  $\rightarrow$  I transition is so slow that the coexistence of nematic phase and isotropic phase inside the gel can be observed during swelling process. The N  $\rightarrow$  I transition develops from surface toward center of the gel with accompanying swelling, and the completion of the N  $\rightarrow$  I transition at  $T_{I,3}$  requires  $6.9 \times 10^3$  s. After the end of the N  $\rightarrow$  I transition, the totally isotropic gel exhibits further swelling until the equilibrium swelling is achieved. The diameter change in swelling process at each  $T_d$  is displayed in Figure 5a. The data at each  $T_d$  are

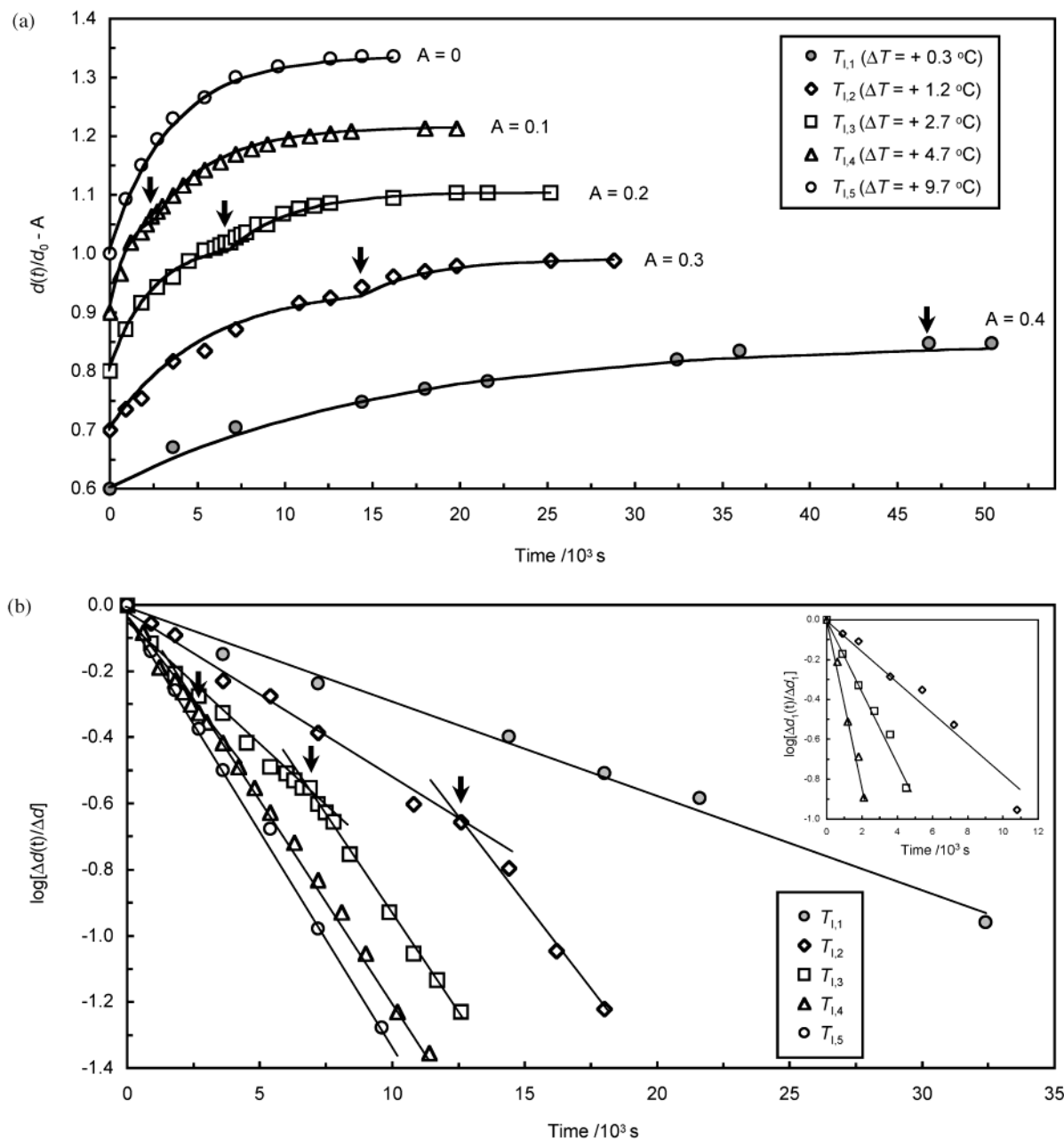


**Figure 5.** Variation of gel diameter in swelling processes accompanying the  $N \rightarrow I$  transition after  $T$ -jumps varying in the distance of  $T_d$  from  $T_{NI}^G$  ( $\Delta T$ ): (a) The time dependence of  $d(t)/d_0$  where  $d_0$  is the equilibrium diameter at  $T_i = 69.5$  °C. Each swelling curve is vertically shifted by  $A$  to avoid overlapping. (b) Semilog plot of the ratio  $\Delta d(t)/\Delta d$  vs time. The inset shows a semilog plot of the ratio  $\Delta d_1(t)/\Delta d_1$  vs time. The arrows indicate the time  $t_{NI}$  when the nematic phase completely disappears. In the case of  $\Delta T = +9.7$  °C, the  $N \rightarrow I$  transition completes within the  $T$ -jump. The solid lines in (a) represent the curves calculated from eq 5 with the estimated values of  $\tau_1$ ,  $\tau_2$ , and  $t_{NI}$ .

vertically shifted to avoid overlapping. As  $T_d$  is closer to  $T_{NI}^G$ , the time for completion of  $N \rightarrow I$  transition ( $t_{NI}$ ) as well as the time for swelling equilibrium becomes longer. Each swelling curve at  $T_d = T_{l,2}$ ,  $T_{l,3}$ , or  $T_{l,4}$  (case ii) exhibits a kink around  $t_{NI}$  indicated by arrow in the figure. This feature is more clearly visible in a semilog plot of  $\Delta d(t)/\Delta d$  vs  $t$  in Figure 5b as a definite crossover in slope at  $t_{NI}$  for the data of  $T_d = T_{l,2}$ ,  $T_{l,3}$ , or  $T_{l,4}$ . This suggests that the swelling in case ii is composed of the two different stages, i.e., during the  $N \rightarrow I$  transition ( $t < t_{NI}$ ) and after the  $N \rightarrow I$  transition ( $t > t_{NI}$ ). The total swelling process in case ii may be expressed as a sum of the two processes, each of which is approximated by a single-exponential relaxation:

$$d(t) = d_0 + \Delta d_1(t) + H(t - t_{NI})\Delta d_2(t) \quad (5)$$

where

$$\Delta d_1(t) = d^* - d(t) = \Delta d_1 \left\{ 1 - \exp\left(-\frac{t}{\tau_1}\right) \right\} \quad (6)$$

$$\Delta d_2(t) = d_\infty - d(t) = \Delta d_2 \left\{ 1 - \exp\left(-\frac{t - t_{NI}}{\tau_2}\right) \right\} \quad (7)$$

and  $H(x)$  is the Heaviside step function defined as  $H(x) = 1$  for  $x \geq 0$  and  $H(x) = 0$  for  $x < 0$ . Each of  $\Delta d_1$  and  $\Delta d_2$  corresponds to the total diameter change in each process:

$$\Delta d_1 = d^* - d_0 \quad (8)$$

$$\Delta d_2 = d_\infty - d^* \quad (9)$$

where  $d^*$  is the gel diameter at  $t_{NI}$ . The inset in Figure 5c illustrates the semilog plots of  $\Delta d_1(t)/\Delta d_1$  vs time for the data of  $T_d = T_{1,2}, T_{1,3}, T_{1,4}$  at  $t < t_{NI}$ . The good linear correlation indicates that the swelling during the  $N \rightarrow I$  transition obeys a single-exponential relaxation process;  $\tau_1$  for each  $T_d$  is estimated from each gradient. The value of  $\tau_2$  is evaluated from the slope at  $t > t_{NI}$  in Figure 5b which is identical with the slope in a semilog plot for  $\Delta d_2(t)/\Delta d_2$  vs  $(t - t_{NI})$ . The values of  $\tau_1$  and  $\tau_2$  for each  $T_d$  are tabulated in Table 1. The swelling curves calculated from eq 5 using the  $\tau_1$  and  $\tau_2$  values, represented by solid lines in Figure 5a, fit the data. For the data at  $T_{1,5}$  (case i), we set  $t_{NI} = 0$  and  $d^* = d_i$ .

Figure 6 shows the Arrhenius plots of  $\tau_1^{-1}$ ,  $\tau_2^{-1}$ , and  $t_{NI}^{-1}$  vs  $T_d^{-1}$  in case ii. It is found that  $\tau_1$  and  $t_{NI}$  are  $T$ -dependent; the  $T$  dependence of  $\tau_1^{-1}$  and  $t_{NI}^{-1}$  obeys the Arrhenius type. In addition, the values of the ratio  $t_{NI}/\tau_1$  (2.7, 2.8, and 2.5 for  $T_{1,2}, T_{1,3}$ , and  $T_{1,4}$ , respectively) are almost constant independently of  $T_d$ . These results suggest that the swelling process at  $t < t_{NI}$  is a thermally activated process which is strongly correlated with the  $N \rightarrow I$  transition. The ratio  $t_{NI}/\tau_1$  ( $\approx 3$ ) is close to the ratio of the relaxation time to the equilibration time for typical single-exponential relaxation, which ensures that  $t_{NI}$  corresponds to the equilibration time for the first swelling process at  $t < t_{NI}$ . The activation energy for the  $N \rightarrow I$  transition ( $E_a$ ) in case ii is evaluated from the Arrhenius plot of  $t_{NI}$  as  $E_a = 4.8 \times 10^5$  J/mol. This value is 2 orders of magnitude larger than transition heats of usual nematic LCs. It should be recalled that the  $N \rightarrow I$  transition of a nematic gel surrounded by solvent can be caused not only by temperature but also by the dilution of network nematicity due to swelling. When the latter effect becomes significant, the  $N \rightarrow I$  transition is decelerated because the swelling is driven by collective diffusion of network. Thus, the activation energy for the  $N \rightarrow I$  transition coupled with swelling apparently becomes much higher than that for  $N \rightarrow I$  transitions in pure LC systems or LC mixture systems with fixed compositions.

In contrast,  $\tau_2$  for the second swelling process at  $t > t_{NI}$  is independent of  $T_d$ . Further, as seen in Table 1, the  $D$  values at  $t > t_{NI}$  in case ii are comparable to  $D$  for the swelling within isotropic phase as well as  $D$  in case i. This clearly demonstrates that the second swelling process at  $t > t_{NI}$  is substantially the same as the swelling process of totally isotropic gel.

In the case of the  $T$ -jump to the temperature slightly above  $T_{NI}^G$  (case iii), the swelling is also coupled with the  $N \rightarrow I$  transition, but the dynamics is significantly different from that in case ii. As can be seen in Figure 4c, the  $N \rightarrow I$  transition tends to begin from edges or scratches on gel surface; both the  $N \rightarrow I$  transition and swelling progress nonuniformly. The boundary between nematic and isotropic phases inside the gel as well as the outline of the gel is considerably rough during the swelling process, particularly at the early stage. The swelling is equilibrated at almost the same time as the nematic phase disappears completely. Because of the rough outline of the gel,  $d(t)$  was obtained by averaging the diameters over the whole gel. It is seen in Figure 5a,b that the transition in case iii is markedly slower than those in other cases; the swelling process is well

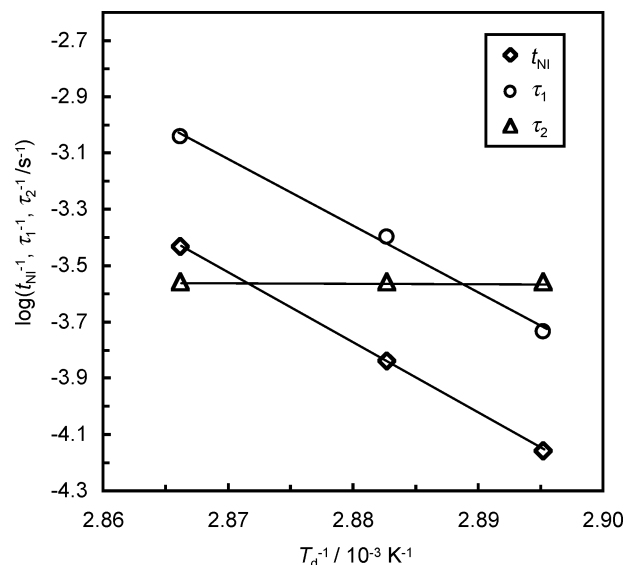


**Figure 6.** Arrhenius plots of  $\tau_1^{-1}$ ,  $\tau_2^{-1}$ , and  $t_{NI}^{-1}$  vs  $T_d^{-1}$  for the swelling processes at  $T_{1,2}$ ,  $T_{1,3}$ , and  $T_{1,4}$  corresponding to case ii. The slope of the line for  $t_{NI}^{-1}$  yields  $E_a = 4.8 \times 10^5$  J/mol as the activation energy for the  $N \rightarrow I$  transition coupled with swelling in case ii.

described by a single-exponential relaxation. The swelling curve for  $T_{1,1}$  in Figure 5a was calculated using eq 5 with  $d^* = d_\infty$ . The value of  $D$  ( $= 4.30 \times 10^{-9}$  cm<sup>2</sup>/s) in case iii is much smaller than  $D$  ( $= 2.35 \times 10^{-8}$  cm<sup>2</sup>/s) in case i without coupling with the  $N \rightarrow I$  transition. It is expected that in case iii where  $\Delta T$  is very small the change in free energy applied by temperature is not definitely larger than  $E_a$  in case ii; the resulting  $N \rightarrow I$  transition is triggered by heterogeneous nucleation. The onset of such  $N \rightarrow I$  transition is susceptible to the edges or scratches on gel surface where the nucleation energy is relatively lowered. The heterogeneous nucleation for the  $N \rightarrow I$  transition and the following growth process of isotropic domains yield nonuniform swelling because the isotropic part swells whereas the nematic part remains shrunken.

**Kinetics of Shrinking Induced by  $I \rightarrow N$  Transition.** We mention here the transition kinetics from the swollen isotropic state to the shrunken nematic state. The initial temperature was fixed at  $T_i = T_{NI}^G + 0.6$  °C. The quench depth, i.e., the distance of  $T_d$  from  $T_{NI}^G$  ( $\Delta T$ ), was varied as  $\Delta T = -0.3, -6.9$ , and  $-14.7$  °C, and the corresponding  $T_d$  was designated as  $T_{N,i}$  ( $i = 1-3$ ) in order of  $\Delta T$  as shown in Figure 2. Qualitatively, the appearance of the  $I \rightarrow N$  transition observed is categorized into the two types, depending on  $\Delta T$ :  $T_d$  sufficiently far from  $T_{NI}^G$  ( $T_{N,2}, T_{N,3}$ );  $T_d$  slightly below  $T_{NI}^G$  ( $T_{N,1}$ ).

Parts a and b of Figure 7 show the optical micrographs for the shrinking processes after the sufficiently deep quench to  $T_{N,2}$  and the shallow quench to  $T_{N,1}$ , respectively. At  $T_{N,2}$ , the cross-polarized image of the gel becomes brighter with time over the whole gel. The nematic ordering and shrinking appear to proceed uniformly. The time at the completion of the  $I \rightarrow N$  transition ( $t_{IN}$ ) is almost the same as the equilibration time for shrinking, although the evaluation of  $t_{IN}$  involves some uncertainty in determining when the appearance of nematic phase shows no further change. The transition process at  $T_{N,3}$  ( $< T_{N,2}$ ) is apparently similar to that at  $T_{N,2}$ , although the pictures are not displayed here. The shrinking curves and semilog plots

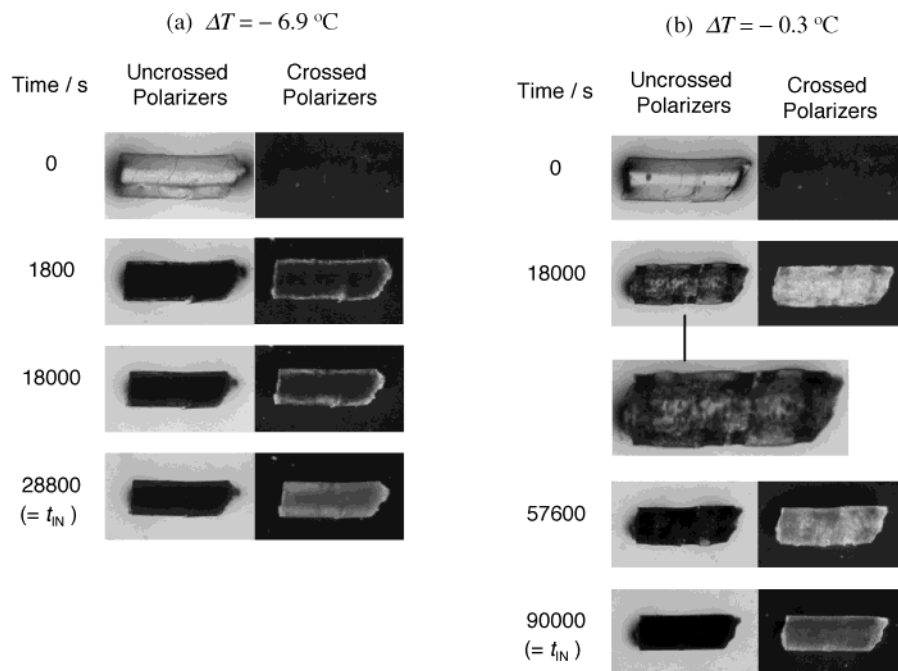


**Figure 7.** Optical micrographs of the gel in shrinking processes accompanying  $I \rightarrow N$  transition after  $T$ -quenches varying in the distance of  $T_d$  from  $T_{NI}^G$  ( $\Delta T$ ): (a)  $\Delta T = -6.9$  °C; (b)  $\Delta T = -0.3$  °C. In (b), the outline of the gel as well as the boundary between nematic and isotropic domains is markedly rough particularly at the early stage, as shown in the enlarged photograph.

of  $\Delta d(t)/\Delta d$  vs  $t$  at  $T_{N,2}$  and  $T_{N,3}$  are illustrated in parts a and b of Figure 8, respectively. As seen in Figure 8b and Table 1, almost the whole shrinking process at  $T_{N,2}$  or  $T_{N,3}$  is expressed by a single-exponential relaxation, but the  $D$  value at  $T_{N,2}$  is fairly smaller than that at  $T_{N,3}$ . There exist the large differences in applied quench depth ( $\Delta T$ ) and degree of volume change ( $\gamma_V$ ) between the shrinking at  $T_{N,2}$  and  $T_{N,3}$ . To examine the former effect, we have compared the shrinking kinetics of LCN-B after the quenches to  $T'_{N,1} = T_{NI}^G - 0.9$  °C and  $T'_{N,2} = T_{NI}^G - 7.8$  °C from  $T_i = T_{NI}^G + 1.1$  °C. As can be seen in Figure 2, this comparison enables us to discuss purely the quench depth effect due to almost the same  $\gamma_V$  in both quenches. As is evident in Figure 8c, the shrinking rates of LCN-B at  $T'_{N,1}$  and  $T'_{N,2}$  are almost identical, and the estimated values of  $D$  for  $T'_{N,1}$  and  $T'_{N,2}$  are  $2.81 \times 10^{-9}$  cm<sup>2</sup>/s and  $2.65 \times 10^{-9}$  cm<sup>2</sup>/s, respectively.<sup>26</sup> This obviously indicates that  $\Delta T$  has no significant influence on shrinking kinetics when  $\Delta T$  is sufficiently large. It was reported for poly(*N*-isopropylacrylamide) (PNIPA) gels that  $D$  for shrinking process accompanied by phase separation decreased with increasing  $\gamma_V$  when  $\gamma_V$  was large.<sup>20</sup> Thus, the considerably smaller  $D$  for the shrinking of LCN-A at  $T_{N,2}$  relative to  $T_{N,3}$  is primarily attributed to the larger  $\gamma_V$  at  $T_{N,2}$ . It is also noticed in Figure 8 that a considerably first shrinking process exists at short time region near  $t = 0$  in the case of the sufficiently large  $T$  quenches. This is recognized as a finite intercept at  $t = 0$  of each linear extrapolation line in Figure 8b,c as well as a fairly large drop in  $d$  at short times near  $t = 0$  in Figure 8a. Because of the presence of this first shrinking mode, the whole shrinking processes after the sufficiently large quenches are not well described by a single-exponential relaxation.

In the case of the shallow quench to  $T_{N,1}$ , the  $I \rightarrow N$  transition and shrinking proceed nonuniformly as shown in Figure 7b. The situation is qualitatively similar to the nonuniform  $N \rightarrow I$  transition and swelling after the  $T$ -jump to  $T_{i,1} \approx T_{NI}^G$  in Figure 4c, although the

direction of the transition is opposite. The onset of the  $I \rightarrow N$  transition is susceptible to edges or scratches on gel surface. The outline of the gel in the initial shrinking process is appreciably rough. The cross-polarized image of the gel at the early stage appears to be brighter than that at the later stage. Although the origin of such brightness change in the cross-polarized image is not clear at present, it may reflect the size growth of constituent nematic domain of polydomain structure. Otherwise, in the beginning of heterogeneous nematic ordering, only the surface area is nematic whereas the inner part of gel remains isotropic and transparent, which may transmit more light than the further shrunken gel with a developed polydomain nematic structure with random orientation of directors. The shrinking reaches equilibrium at almost the same time as the  $I \rightarrow N$  transition ends. As is obvious from Figure 8a, the transition after the shallow quench is much slower than that after the deep quenches. The values of  $d(t)$  for the gel with rough outline were obtained by averaging the diameters over the whole gel. As seen in Figure 8b, the shrinking process at  $T_{N,1}$  is almost approximated by a single-exponential relaxation. The data at long times appear to deviate from the linear extrapolation, which may imply that the shrinking obeys another type of relaxation process such as the Avrami equation ( $d(t) \sim t^n$ ). However, the single-exponential approximation is more or less tolerable here to focus on the comparison of  $\tau$  at different  $T_d$ . The estimated  $D$  ( $= 1.26 \times 10^{-9}$  cm<sup>2</sup>/s) at  $T_{N,1}$  is significantly smaller than that ( $= 4.70 \times 10^{-9}$  cm<sup>2</sup>/s) at  $T_{N,2}$ , although the  $\gamma_V$  values at  $T_{N,1}$  and  $T_{N,2}$  are comparable. The markedly small  $D$  at  $T_{N,1}$  is attributed to the nonuniform processes of shrinking and  $I \rightarrow N$  transition. The nonuniform nematic ordering and shrinking caused by the shallow quench have essentially the same origin as the nonuniform  $N \rightarrow I$  transition and swelling after the  $T$ -jump to  $T_{i,1} \approx T_{NI}^G$  as described before: The free energy change given by the shallow quench is not enough to drive the homogeneous nematic ordering,

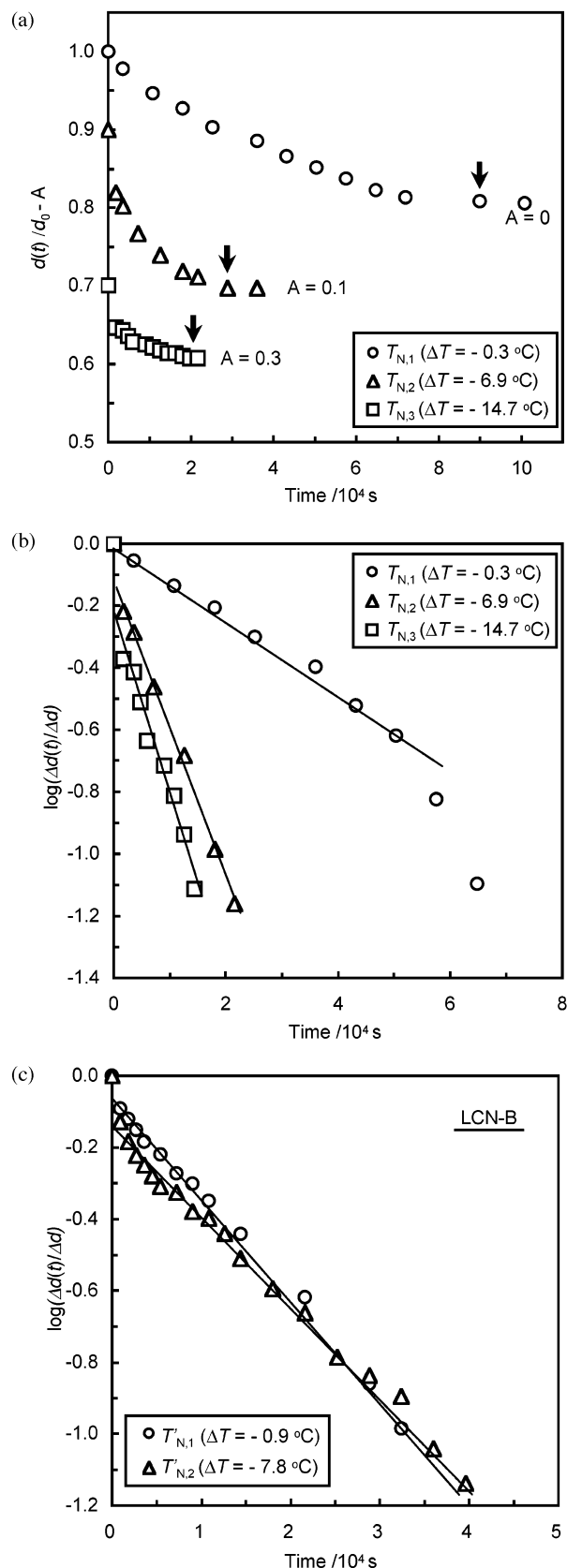


**Figure 8.** Variation of gel diameter in shrinking processes accompanying the I → N transition after  $T$ -quenches varying in the distance of  $T_d$  from  $T_{NI}^G$  ( $\Delta T$ ): (a) The time dependence of  $d(t)/d_0$  where  $d_0$  is the equilibrium diameter at  $T_i = 71.5$  °C. Each data are vertically shifted by  $A$  to avoid overlapping. The arrows indicate the time  $t_N$  when I → N transition ends. (b) Semilog plot of the ratio  $\Delta d(t)/\Delta d$  vs time. (c) Comparison of the shrinking processes of LCN-B after  $T$ -quenches across  $T_{N,1}$  and  $T_{N,2}$ , yielding almost the same volume change.

which yields the nematic ordering caused by heterogeneous nucleation; the following growth of the nematic nuclei results in nonuniform shrinking.

It is noticed in Table 1 that each of the  $D$  values for the swelling induced by the N → I transition and the shrinking induced by the I → N transition is roughly summarized as the order of  $10^{-8}$  or  $10^{-9}$  respectively, except for the cases of  $T_d \approx T_{NI}^G$ ; as a whole, the latter process is considerably slower than the former. The slightly higher viscosity of the solvent in nematic phase than that in isotropic phase acts to retard the shrinking process from isotropic gel to nematic gel, but the effect will be minor. It should be recalled that even within the nematic phase,  $D$  for shrinking is significantly smaller than that for swelling. The shrinking involving the formation (or re-formation) process of the single nematic phase inside gel requires long time. This is qualitatively similar to volume phase transition of PNIPA gels where the shrinking process is strongly decelerated in comparison with the swelling process due to the phase separation and the following homogenization processes.<sup>16–20</sup>

## Summary

The kinetics of the phase transition from shrunken nematic gel to swollen isotropic gel after  $T$ -jumps across  $T_{NI}^G$  primarily depends on  $\Delta T$ , i.e., the distance of  $T_d$  from  $T_{NI}^G$ . When  $\Delta T$  is sufficiently large, the N → I transition completes fast, and the total swelling process is identical with that of the isotropic gel without the N → I transition. If  $\Delta T$  is moderately small, the swelling coupled with the N → I transition appears. Such N → I transition slowly develops from surface toward center of gel with accompanying swelling, and thereafter the totally isotropic gel swells further. The activation energy of the N → I transition coupled with swelling is 2 orders of magnitude larger than transition heat of usual bulk LC because the transition is markedly retarded by swelling, i.e., collective diffusion of network.

When the depth of  $T$ -quench from nematic phase to isotropic phase is sufficiently large, the formation of nematic phase inside gel as well as the shrinking progresses uniformly. The rate of the shrinking accompanying nematic ordering primarily depends on the degree of total volume change but not on the depth of  $T$ -quench.

If  $T_d$  is slightly above (or below  $T_{NI}^G$ ), the onset of the N → I (or I → N) transition is triggered by heterogeneous nucleation. The following growth of isotropic (or nematic) domains results in significantly nonuniform swelling (or shrinking). As a result, the phase transitions at  $T_d \approx T_{NI}^G$  are remarkably decelerated compared to those caused by the  $T$ -jumps with sufficiently large  $\Delta T$ .

**Acknowledgment.** The authors are grateful to Prof. Hiromu Saito at Tokyo University of Agriculture and Technology for valuable discussions. Y. O. Arai expresses her thanks to the Research Fellowships of the Japan Society for the Promotion of Science (JSPS). This work is partly supported by a Grant-in-Aid for JSPS Fellows (No. 15005225).

## References and Notes

- (1) Brand, H. R.; Finkelmann, H. In *Handbook of Liquid Crystals*; Demus, D., et al., Eds.; Wiley-VCH: Weinheim, 1998; Vol. 3.

- (2) Warner, M.; Terentjev, E. M. *Liquid Crystal Elastomers*; Oxford University Press: Oxford, 2003.
- (3) Urayama, K.; Okuno, Y.; Kawamura, T.; Kohjiya, S. *Macromolecules* **2002**, *35*, 4567.
- (4) Urayama, K.; Okuno, Y.; Kohjiya, S. *Macromolecules* **2003**, *36*, 6229.
- (5) Urayama, K.; Okuno, Y.; Nakao, T.; Kohjiya, S. *J. Chem. Phys.* **2003**, *118*, 2903.
- (6) Okuno, Y.; Urayama, K.; Kohjiya, S. *J. Chem. Phys.* **2003**, *118*, 9854.
- (7) Wang, X. J.; Warner, M. *Macromol. Theory Simul.* **1997**, *6*, 37.
- (8) Matsuyama, A.; Kato, T. *J. Chem. Phys.* **2002**, *116*, 8175.
- (9) Nakai, A.; Shiwa, T.; Wang, W.; Hasegawa, H.; Hashimoto, T. *Macromolecules* **1996**, *29*, 5990.
- (10) Dorgan, J. R.; Yan, D. *Macromolecules* **1998**, *31*, 193.
- (11) Fukuda, J. *Phys. Rev. E* **1999**, *59*, 3275.
- (12) Nwabunma, D.; Kyu, T. *Macromolecules* **1999**, *32*, 664.
- (13) Matsuyama, A.; Kato, T. *J. Chem. Phys.* **2000**, *113*, 9300.
- (14) Kim, D.; Kyu, T. *J. Polym. Sci., Part B: Polym. Phys.* **2003**, *41*, 913.
- (15) Tanaka, T.; Sato, E.; Hirokawa, Y.; Hirotsu, S.; Peetermans, J. *Phys. Rev. Lett.* **1985**, *55*, 2455.
- (16) Hirose, H.; Shibayama, M. *Macromolecules* **1998**, *31*, 5336.
- (17) Shibayama, M.; Nagai, K. *Macromolecules* **1999**, *32*, 7461.
- (18) Suzuki, A.; Yoshikawa, S.; Bai, G. *J. Chem. Phys.* **1999**, *111*, 360.
- (19) Takigawa, T.; Yamawaki, T.; Takahashi, K.; Masuda, T. *Polym. J.* **1999**, *31*, 595.
- (20) Takahashi, K.; Takigawa, T.; Masuda, T. *J. Chem. Phys.* **2004**, *120*, 2972.
- (21) Yusuf, Y.; Ono, Y.; Sumisaki, Y.; Cladis, P. E.; Brand, H. R.; Finkelmann, H.; Kai, S. *Phys. Rev. E* **2004**, *69*, 021710.
- (22) The change of  $d_{\text{dry}}$  in response to  $T$  variation is negligibly small (less than 0.5%) in the  $T$  range from 45 to 140 °C. Thus, the volume change in Figure 2 is entirely attributed to the change of solvent content in gel.
- (23) Onuki, A. *Adv. Polym. Sci.* **1993**, *109*, 63.
- (24) Chandrasekhar, S. *Liquid Crystals*; Cambridge University Press: Cambridge, 1992.
- (25) de Gennes, P. G.; Prost, J. *The Physics of Liquid Crystals*, 2nd ed.; Oxford University Press: Oxford, 1993.
- (26) A finite difference in  $D$  for shrinking between LCN-A at  $T_{N,2}$  and LCN-B at  $T_{N,2}$  ( $\approx T_{N,2}$ ) will originate from the difference of the samples prepared separately.

MA049175+